

Research Paper

Development of Experimental P-Y Curves from Centrifuge Tests for Piles Subjected to Static Loading and Liquefaction-Induced Lateral Spreading

Milad Souri^{1*}, Arash Khosravifar², Scott Schlechter³, Nason McCullough⁴, and Stephen E. Dickenson⁵

Abstract: The results of five centrifuge models were used to evaluate the response of pile-supported wharves subjected to inertial and liquefaction-induced lateral spreading loads. The centrifuge models contained pile groups that were embedded in rockfill dikes over layers of loose to dense sand and were shaken by a series of ground motions. The p-y curves were back-calculated for both dynamic and static loading from centrifuge data and were compared against commonly used American Petroleum Institute p-y relationships. It was found that liquefaction in loose sand resulted in a significant reduction in ultimate soil resistance. It was also found that incorporating *p*-multipliers that are proportional to the pore water pressure ratio in granular materials is adequate for estimating pile demands in pseudo-static analysis. The unique contribution of this study is that the piles in these tests were subjected to combined effects of inertial loads from the superstructure and kinematic loads from liquefaction-induced lateral spreading.

Keywords: pile foundations; liquefaction; lateral spreading; centrifuge models; p-y curves

Introduction

Liquefaction-induced ground deformations can cause severe damage to pile-supported wharves and other waterfront structures. A common approach in analyzing the lateral behavior of piles against seismic loads is using the beam on nonlinear Winkler foundation (BNWF) simulation or p-y spring analysis. One common p-y relationship for sand is the one proposed by the American Petroleum Institute, also known as the API sand model (API 1993). While the API sand model was originally developed for static loading conditions, it is common to modify the API sand curves to account for the effects of cyclic loading. A number of studies have shown that complex pile behavior under dynamic loading conditions is not captured by the API curves. Observations from a series of dynamic centri-

fuge tests reported by Wilson (1998) indicate that peak values of soil reaction for the experimentally derived p-y curves were significantly greater than those recommended by the API p-y curve at depths that are less than approximately three times the pile diameter. Yang et al. (2011) performed a series of shaking table tests on dry and saturated dense sand deposits and found that the API p-y curve underpredicts the ultimate soil resistance (smaller than one third of experimental p-y curves) at shallow depths. Yoo et al. (2013) carried out a centrifuge test for a single pile in dry sand under sine wave loading and found that pseudo-static analysis using the API curve overestimated the maximum bending moment and pile displacements as compared to those measured from the centrifuge test. They also found that the subgrade reaction modulus at shallow depths could be overestimated by the API sand curve within an elastic pile displacement of 1% of the pile diameter. On the other hand, when the displacement of the pile was greater than 1% of the pile diameter, which may occur during earthquake loading, the API sand relation significantly underestimated the ultimate soil reaction at shallow depths.

Existing p-y curves have been widely used in pseudo-static analysis to predict the response of pile foundations in liquefied soils. However, there is no consensus on how to modify the static p-y curves to account for the effects of liquefaction and pore water pressure generation in loose granular soils. In previous studies, the p-y springs of piles in liquefying soils were back-calculated from case histories, centrifuge model studies (e.g., Wilson *et al.* 2000; Brandenberg *et al.* 2005; Abdoun *et al.* 2003), full-scale tests (e.g., Rollins *et al.* 2005; Chang and Hutchinson 2013), and numerical analyses (e.g., McGann *et al.* 2011).

Graduate Student Researcher, Department of Civil and Environmental Engineering, Portland State University, 1930 SW 4th Ave, Portland, OR, 97201, USA

Assistant Professor, Department of Civil and Environmental Engineering, Portland State University, Portland, 1930 SW 4th Ave, Portland, OR, 97201, USA

³ Principal, GRI, Beaverton, OR, USA

⁴ Principal Geotechnical Engineer, Jacobs Engineering Group, 1100 NE Circle Blvd Suite 300, Corvallis, OR, 97330, USA

Principal Engineer, New Albion Geotechnical, Inc.,
3400 San Juan Dr, Reno, NV, 89509, USA

Corresponding author, email: msouri@pdx.edu

© 2020 Deep Foundations Institute, Print ISSN: 1937-5247 Online ISSN: 1937-5255 Published by Deep Foundations Institute Received 20 November 2019; received in revised form 20 April 2020; accepted 12 May 2020 https://doi.org/10.37308/DFI|nl.20191120.212

One approach to account for the effect of partial/full liquefaction on the p-y curve is to apply a p-multiplier to degrade the ultimate soil resistance of liquefied soil. Liu and Dobry (1995) investigated the effect of excess pore water pressure on the p-y curve in partially/fully liquefied sands by performing a series of centrifuge tests, and they defined a dimensionless degradation parameter, C_n, that changes more or less linearly with the excess pore water pressure ratio R_{ij} to degrade the p-y curves. Wilson (1998) performed a series of dynamic centrifuge tests in complement with pseudo-static analyses of pile-supported structures. They concluded that the p-multiplier strongly correlated to initial relative density (D_p) of the soil. They found that a range of 0.1–0.2 for relatively loose sand ($D_R = 35\%$) and about 0.25–0.35 for medium dense sand ($D_R = 55\%$) would be reasonable to predict the measured pile demands. Tokimatsu (1999) evaluated the field performance of pile foundations subjected to lateral ground spreading during the 1995 Kobe earthquake. They compared the pseudo-static analysis results to values in well-documented case histories and concluded that p-multipliers ranging from 0.05 to 0.2 are reasonable for predicting the observed pile performance in liquefied soils in the field.

Another approach proposed in other studies uses an upward concave shape for p-y curves in liquefied soils (e.g., Rollins et al. 2005; Franke and Rollins 2013; Chang and Hutchinson 2013). Rollins et al. (2005) performed full-scale tests on a large drilled shaft using blast-induced liquefaction, and they proposed an upward concave shape for the p-y curve to capture the dilative behavior of liquefied soils during shearing. Reasonably good agreement was demonstrated between measured and predicted pile response by implementing the proposed p-y curve in the lateral pile analysis. Franke and Rollins (2013) developed a simplified hybrid p-y model by incorporating aspects of the p-y curve of Rollins et al. (2005) and the p-y curve for liquefied soils proposed by Wang and Reese (1998); they evaluated the applicability of the proposed hybrid model against various published case histories and observed a reasonable computed response for piles in liquefied soils under both kinematic and inertial loadings. Chang and Hutchinson (2013) conducted sequential loading on a single-pile specimen in a saturated sand deposit and observed an inverted S-shaped p-y curve from the back-calculated experimental data even at low levels of pore water pressure ratios ($R_{\rm u} > 10-15\%$).

The studies mentioned above provide varying and sometimes contradicting recommendations on how to modify the static p-y curves to capture the complex behavior of soil during the liquefaction process, which highlights the need for further investigation. The focus of this study is to evaluate the effectiveness of the p-multiplier approach in modifying p-y springs in partially/fully liquefied soils to predict the lateral response of piles. This was done by using the results of five centrifuge tests that simulate pile-supported wharves in sloping ground (McCullough *et al.*, 2001). The p-y curves were back-calculated in loose sands, dense sands and sloping rockfill dikes. The p-y curves were back-calculated for both piles subjected to cyclic static push/pull forces at the pile head as

well as for piles subjected to dynamic transient earthquake shaking. The static p-y curves were approximated using the API relationships for sands, and the input parameters for the API curves were back-calculated. The dynamic p-y curves were compared against the static p-y curves to provide insight on the applicability of the p-multiplier approach in developing p-y curves for liquefied zones. What differentiates this study from previous studies on piles in liquefied soils is that the piles in these centrifuge tests were subjected to both kinematic loads from laterally spreading soils as well as inertial loads from the superstructure mass. Therefore, the back-calculated p-y curves in liquefied zones represent a more realistic loading condition for pile-supported structures. To evaluate the effectiveness of using p-multipliers in the API sand curves, the piles from the centrifuge tests were modeled in LPILE (version 2016.9.10; Ensoft, Inc.), and the predicted maximum bending moments in each pile were compared against the values measured in the centrifuge tests. It will be shown that the maximum bending demands in piles were reasonably captured using p-multipliers that are proportional to the pore water pressure ratio in partially/fully liquefied zones.

Description of Centrifuge Tests

Centrifuge Models and Cross Sections

Data from a series of five centrifuge tests were analyzed to back-calculate pile lateral behavior (i.e., the p-y springs) for static and dynamic loading conditions. These tests were performed on pile-supported wharves by Dickenson, Mc-Cullough, Schlechter, and coworkers at the UC Davis Center for Geotechnical Modeling (McCullough et al. 2001). These centrifuge models represent the typical layout of major port facilities in California, and the findings can be used to represent other similar pile-supported wharves embedded in rock dikes over native soils and potentially liquefiable artificial fill soils. The cross sections of all models and key soil properties are shown in Figure 1. Uniform fine Nevada was used in all five centrifuge experiments. The sand had a specific gravity of (Gs) 2.67, mean grain size (D₅₀) of 0.15 mm, coefficient of uniformity (Cu) of 1.6, minimum dry unit weight of 13.98 kN/m³, and maximum dry unit weight of 16.76 kN/m³. The parameters discussed in this paper are all in prototype scale unless noted otherwise.

Dynamically Loaded Piles

The wharf deck in these tests was supported by three rows of seven piles (for a total of 21 piles). The pile diameters ranged from 0.38 m to 0.68 m. Each centrifuge model was subjected to a sequence of scaled input motions with the peak base acceleration values ranging from 0.15 g to 0.82 g. The pile group was subjected to the combined effects of inertial and liquefaction-induced kinematic demands during earthquake shaking (these piles are referred to as *dynamic piles*).

Static Cyclically Loaded Piles

Two of the five tests (SMS02 and JCB01) included two single piles that were statically pushed by two to seven cycles of

2 | DFI JOURNAL | VOL. 14 | ISSUE 1

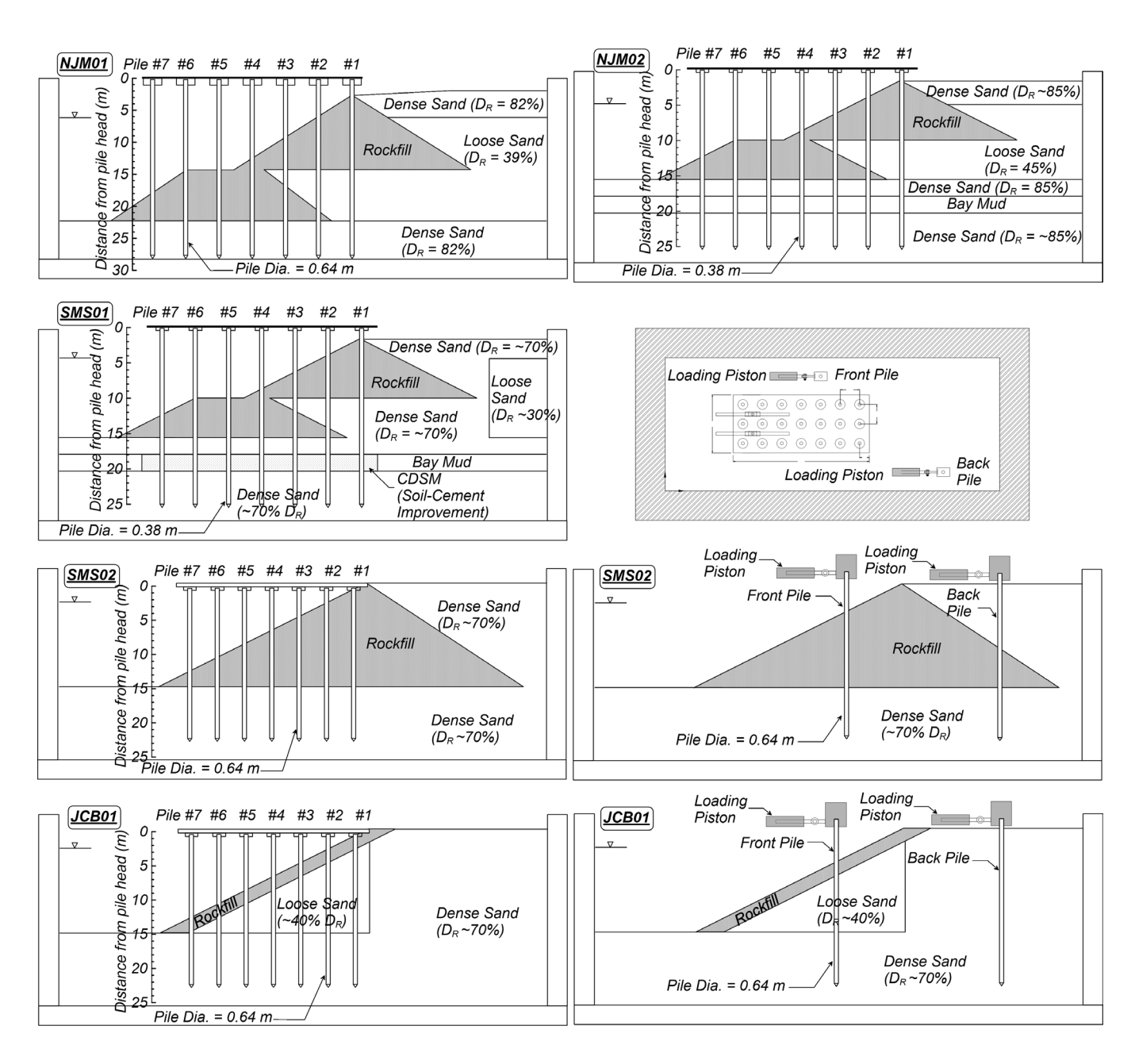


Figure 1. Cross sections and plan view of five centrifuge tests on pile-supported wharves

loads using actuators attached to their pile heads (these piles are referred to as *static piles*). The static loads, which were applied prior to earthquake shaking, provided key data for the comparison of p-y springs under static and dynamic loading conditions. In these two tests, the static pile at the back of the wharf was placed in dense sand with no slope; the static pile at the front of the wharf was placed in sloping rockfill in SMS02 and in a sloping rock face overlying loose sand in JCB01. The layout for the static piles is shown in Figure 1. The structural properties of the static piles were the same as those for the dynamic piles.

Sensors and Instruments

Measurements for all centrifuge tests conducted in this study were obtained using a suite of sensors and instrumentation. Linear volt displacement transducers (LVDT) mounted on the wharf deck, ground surface and the shear box container were used to measure the horizontal and vertical displacements. Pore pressure transducers (PPT) were embedded within the soil model at various depths to measure pore fluid pressures. Accelerometers were embedded within the soil model and attached to the wharf deck and the shear box to measure horizontal ground shaking accelerations. Strain gauges were attached to static and dynamic piles to back-calculate pile bending moments.

Procedures to Back-Calculate P-Y Curves

Lateral Soil Reactions

Bending moments were back-calculated at discrete locations along the pile where strain gauges were attached. The bend-

ing moments were interpolated along the pile length using a cubic spline fitting method before being numerically double-differentiated to back-calculate the lateral soil reactions, p (Haiderali and Madabhushi 2016; Brandenberg *et al.* 2010). For the piles where the bending moment at the pile head was not measured, the bending moments were extrapolated assuming a constant shear force above the ground surface. The bending moments and shear forces at the pile tips were assumed to be zero.

Horizontal Pile Displacements

The horizontal pile displacements were estimated by double-integrating the bending moments along the pile and dividing by the pile flexural stiffness (*EI*). The rotations at the pile head were assumed to be zero as the piles were rigidly connected to a relatively rigid wharf deck. The displacement at the pile head was set to be equal to the measured displacement from the LVDT at the wharf deck and the pile tip was allowed to have a non-zero rotation.

Horizontal Soil Displacements

Total horizontal soil displacements were calculated by combining the transient (high-frequency) and permanent (low-frequency) components of displacement following the methods described by Wilson et al. (2000). Transient soil displacements were calculated by double-integrating the recorded accelerations. A high-pass Butterworth filter was applied to remove the low-frequency motions from the recorded accelerations. The permanent soil displacements were calculated based on the displacements recorded using LVDTs at the ground surface after applying a low-pass Butterworth filter. The pattern of distributing the permanent component of the soil displacement with depth was a major source of uncertainty in our analyses. The estimated pile bending moments in our consecutive pseudo-static analyses were also found to be very sensitive to the assumptions made regarding the pattern of permanent soil displacements with depth, which warranted investigating this issue methodically. After considering various patterns of permanent soil displacement with depth and investigating their effects on the estimated bending moments, we used the normalized shape of the maximum transient soil displacements with depth as a guide to determine where the subsurface shear failure zones formed as well as to distribute the permanent component of the soil displacement from the ground surface down to the shear failure plane. No permanent soil displacement was considered below the shear failure plane.

Back-Calculated P-Y Curves

Lateral pile behavior is commonly characterized using p-y curves at various depths along the pile. The p in these relationships corresponds to the lateral soil reaction, and the y corresponds to the relative displacement between the soil and pile (i.e. y = horizontal pile displacement – horizontal soil displacement). As described earlier, there is some uncertainty in estimating the horizontal soil displacements and pile displacements for dynamic piles. Therefore, the dynamic p-y

curves were used primarily for estimating ultimate lateral soil reaction, and the relative soil—pile displacement (y) was only used qualitatively.

Experimental P-Y Curves from Static Piles

Experimental p-y curves were extracted from the results of statically loaded piles in SMS02 (penetrating dense sand and rockfill) and JCB01 (penetrating dense sand, loose sand and a thin rockfill) prior to shaking. Given that these soil and rockfill units are made from granular materials, the back-calculated p-y curves were approximated using API sand relationships. It was assumed that the behavior of rockfill can be modeled as a granular material; therefore, an API sand with a friction angle was used for rockfill with the properties that are tabulated in Table 1. The API sand model recommends a hyperbolic tangent function to characterize the ultimate soil reaction (p_{ult}) and initial stiffness (k_T) . In the API sand model, the ultimate lateral reaction (p_{ult}) increases with depth, pile diameter and internal friction angle. Internal friction angles of 33°, 37° and 45° were used to develop API curves for loose sand $(D_p = 30\%)$, dense sand $(D_p = 70\% \text{ to } 80\%)$ and rockfill, respectively. It will be discussed later that the API sand models are modified with reduced stiffness for all soil units and a pseudo-cohesion for rockfill to better approximate the p-y curves calculated from the centrifuge tests.

As an example, a comparison between the experimental p-y curve and the API relationship for loose sand is shown in Figure 2a for the front pile in JCB01 at a depth of $3.05 \,\mathrm{m}$, which is approximately five times the pile diameter (D). This static pile was subjected to seven cycles of static loading. Different loading cycles are plotted with different colors on this figure to help understand how p and y evolve in the experimental p-y curve. As can be noticed from this figure, the API sand curve using a friction angle of 33° captures the ultimate resistance of the experimental p-y curve reasonably well. The comparison is not that favorable at other depths; however, it will be shown later that the overall pile demands are reasonably captured using the API sand curves. Figure 2b shows the 6^{th} cycle of the same experimental p-y curve compared to the same API curve used in Figure 2a, which has been manually shifted to the left for plot-

Table 1. Back-calculated input parameters for p-y curves

Soil unit	Total unit weight (kN/m³)	Friction angle	Modeled in <i>LPILE</i>	Modulus of subgrade reaction, k (kN/m³)
Loose sand $(D_R = 30\%$ to 40%)	19.4	33°	API Sand	3500
Dense sand $(D_R = 70\%$ to 85%)	20.4	37°	API Sand	3500
Rockfill	20.5	45°	Cemented c-phi with a pseudo cohesion of 15 kPa	5200

4 | DFI JOURNAL | VOL. 14 | ISSUE 1

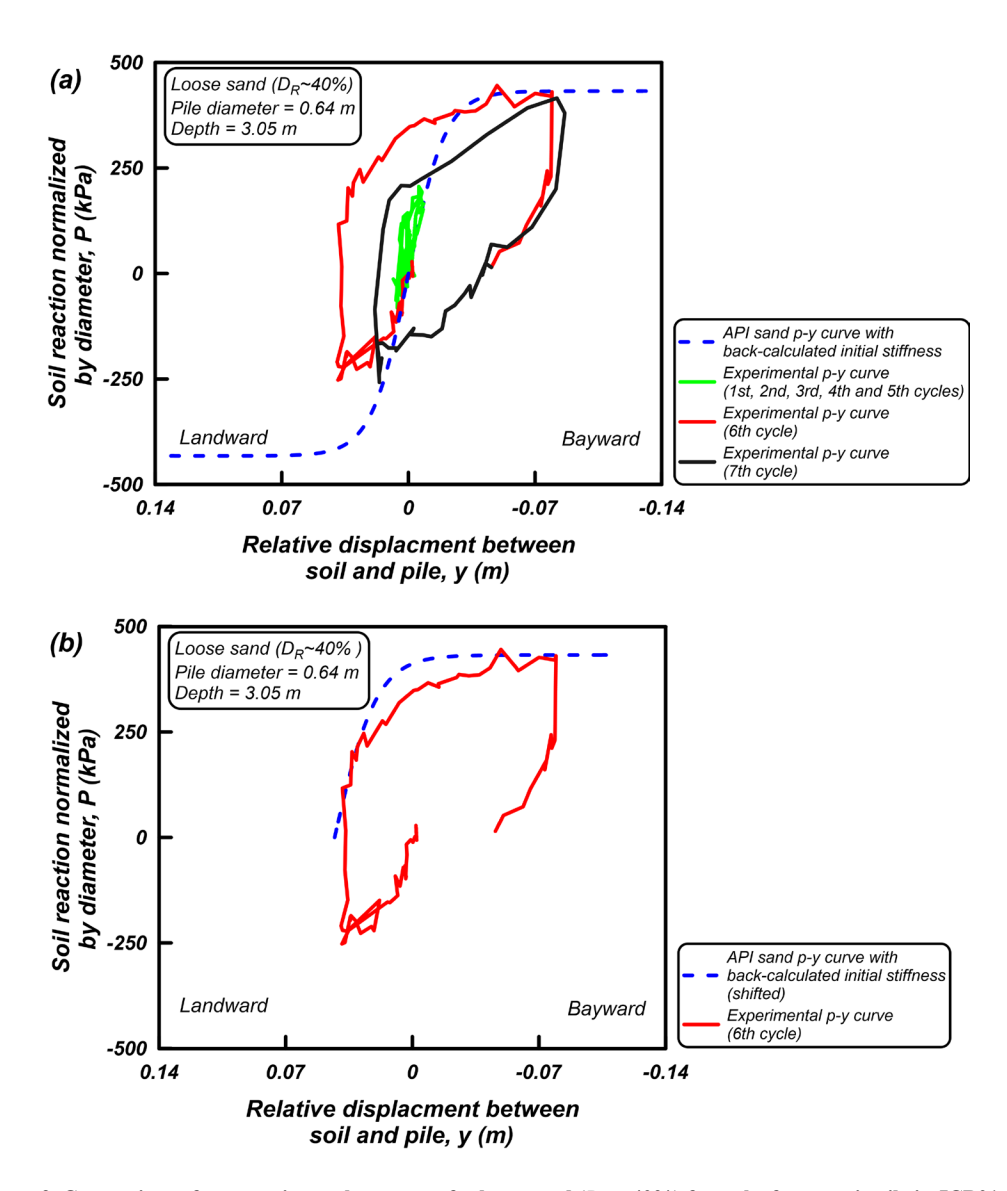


Figure 2. Comparison of an experimental p-y curve for loose sand ($D_R = 40\%$) from the front static pile in JCB01 and API sand using back-calculated input parameters

ting purposes. This figure clearly shows that the API sand curve captures the overall shape of the experimental p-y curve. It will be discussed later how the stiffness of the API sand curves was reduced to better match the experimental results. Similar comparisons were performed for other soil units and at various depths, and these results will be presented next.

Figure 3 presents a comparison between the back-calculated experimental static p-y curves and the API relationships for the back pile and front pile in SMS02 and JCB01 at depths of $\sim 1D$, 3D, 5D and 7D. Comparing the values for ultimate resistance in the API curves with those of the back-calculated p-y curves show that at a depth of $\sim 1D$, the API relationships underestimate the ultimate resistance of the p-y curve. This observation is consistent with the experimental results reported by Wilson (1998) for depths that are less than approximately three times the pile diameter. The comparison is relatively reasonable at depths of 3D to 5D. However, at depths of 5D to 7D, the ultimate resistance values in the experimental curves were not fully mobilized due to small pile deflections.

Modifications to API Sand P-Y Curves

The initial stiffness in the API sand curve (k_T) is the product of the depth below the ground surface and the modulus of the subgrade reaction (k). The initial stiffness in loose sand, dense sand and rockfill were back-calculated from the experimental static p-y curves. The back-calculated initial stiffness values are plotted versus depth in Figure 4. Each data point in this plot represents the initial stiffness calculated from an experimental p-y curve shown in Figure 3. No clear slope effect was observed for the initial stiffness of the p-y curves in the landward and bayward directions for the two front piles in SMS02 and JCB01 located along the face of the rockfill slopes. Therefore, the initial stiffness values plotted in Figure 4 are calculated based on the average values in the landward and bayward directions. These initial stiffness values were then divided by the

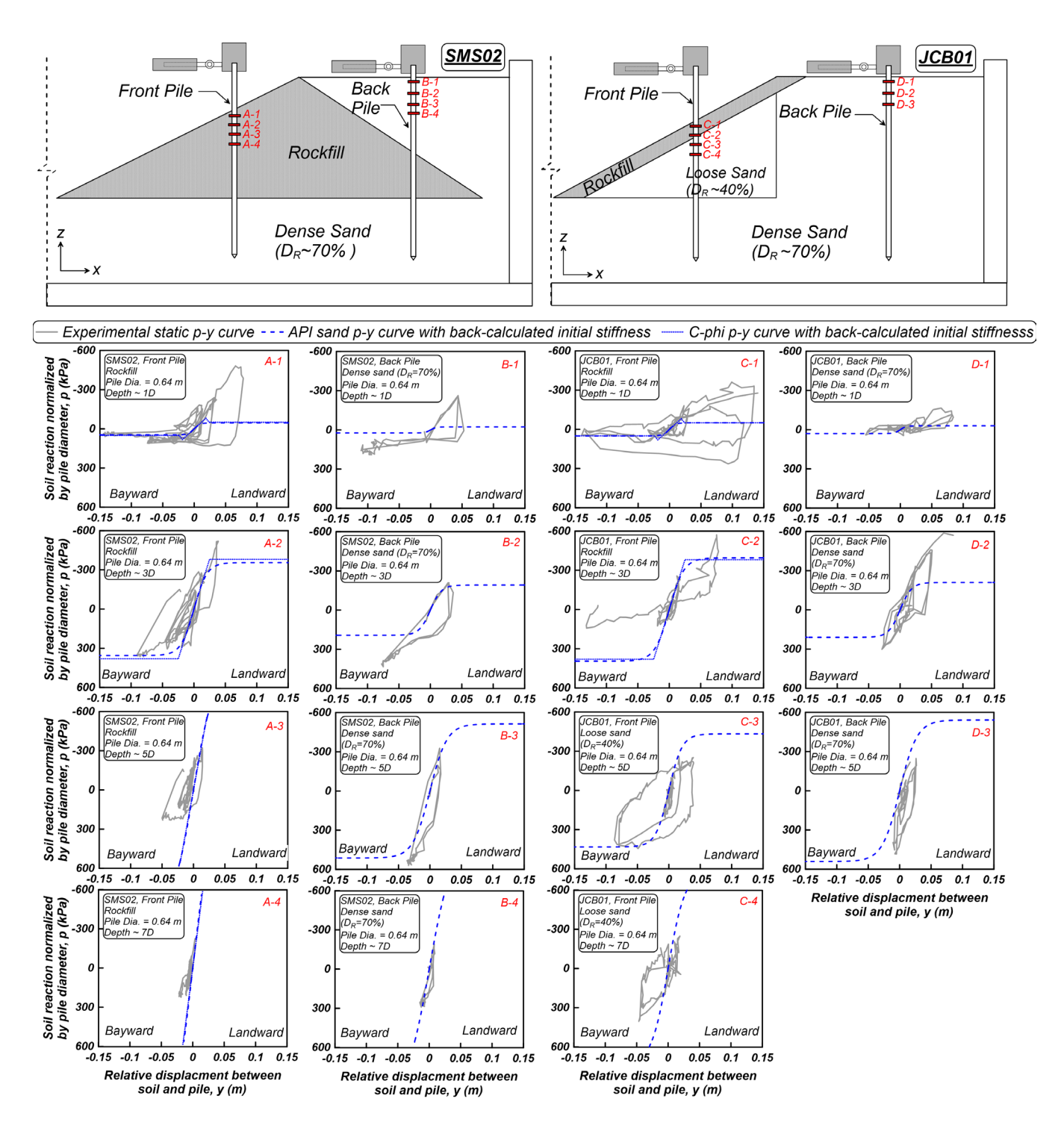


Figure 3. Comparison of experimental p-y curves from static piles in JCB01 and SMS02 and API sand using back-calculated input parameters

corresponding depth to obtain the modulus of subgrade reaction (*k*) for different soil units. The initial stiffness values recommended by API for loose sand, dense sand and rockfill are also plotted in this figure for comparison. It can be observed that the initial stiffness values calculated from experimental p-y curves were smaller than the values recommended by API. This reduction might be attributed to the aging effects between the soils in field and freshly deposited sands in the centrifuge. It could also be due to the uncertainties in back-calculating

the initial stiffness at shallower depths where small variations in the modeling parameters (i.e. friction angle and/or pseudo cohesion for rockfill) may have a large impact. Despite the differences between the back-calculated moduli of subgrade reaction from centrifuge tests and those recommended by API, the results of centrifuge tests are applicable in evaluating the effects of liquefaction on p-y behavior since the comparisons are made between the static and dynamic p-y curves that are driven from the same centrifuge tests.

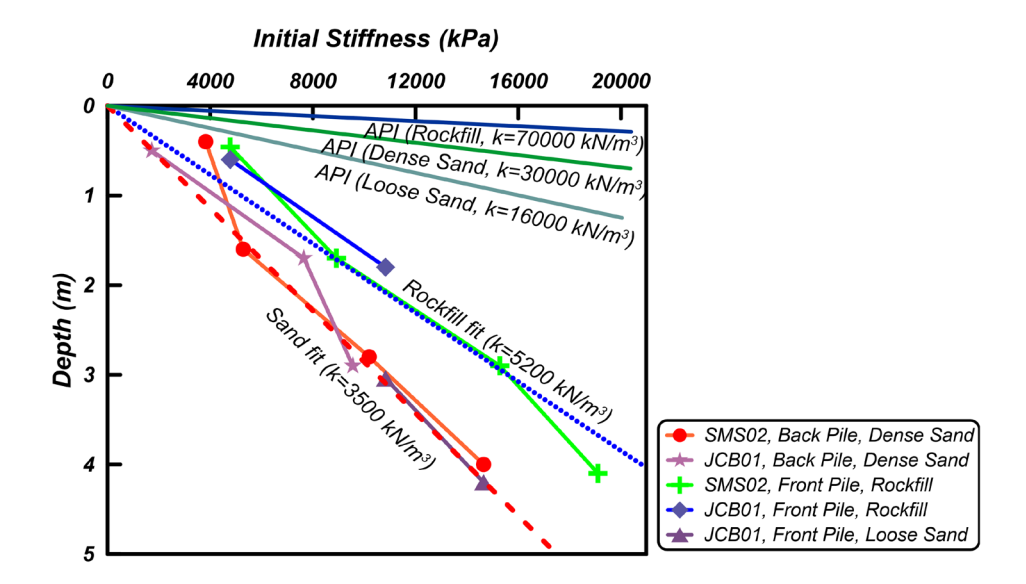


Figure 4. Comparison of initial stiffness back-calculated from experimental static p-y curves and recommended by API

In order to account for additional resistance caused by the interlocking and movement of rock particles near the ground surface, a pseudo-cohesion value of 15 kPa was applied to rockfill as suggested by McCullough and Dickenson (2004). This pseudo-cohesion was incorporated in our analysis by using the cemented c-phi p-y curves implemented in *LPILE*. In the current implementation of the cemented c-phi curves in *LPILE* (version 2016.9.10; Ensoft, Inc.), the difference between API sand and c-phi curves are not significant when the initial stiffness is reduced as evidenced from the p-y curves plotted for rockfill in Figure 3. Table 1 lists the input parameters for p-y curves to approximate the experimental p-y curves from static piles. No significant difference was observed in the back-calculated subgrade reaction moduli between loose and dense sands; therefore, the same modulus is recommended for simplicity.

Validation Using Lateral Pile Response

The effectiveness of the API sand curves in predicting the lateral pile response is investigated by comparing the pile demands measured from static piles in the centrifuge tests to those computed using p-y models in *LPILE*. The shear load and bending moment at the pile head were back-calculated directly from the centrifuge tests and applied as pile head loading conditions in *LPILE*. The p-y curves were developed for loose sand, dense sand, and rockfill based on the input parameters reported in Table 1.

Figure 5 presents the comparison of lateral pile responses measured in the centrifuge and computed using *LPILE* for the front static pile in JCB01, which is selected for comparison purposes because it penetrates through all three soil units and is located on a slope. The *LPILE* results

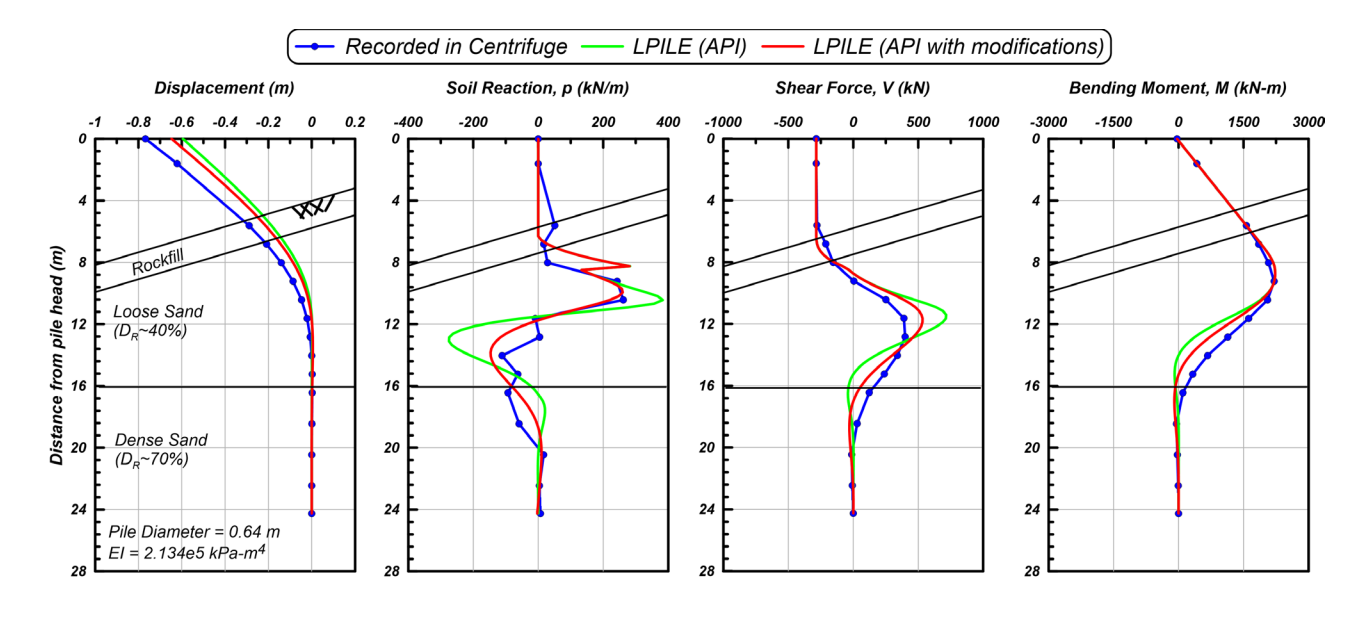


Figure 5. Comparison of recorded and predicted pile lateral responses for the front static pile in JCB01

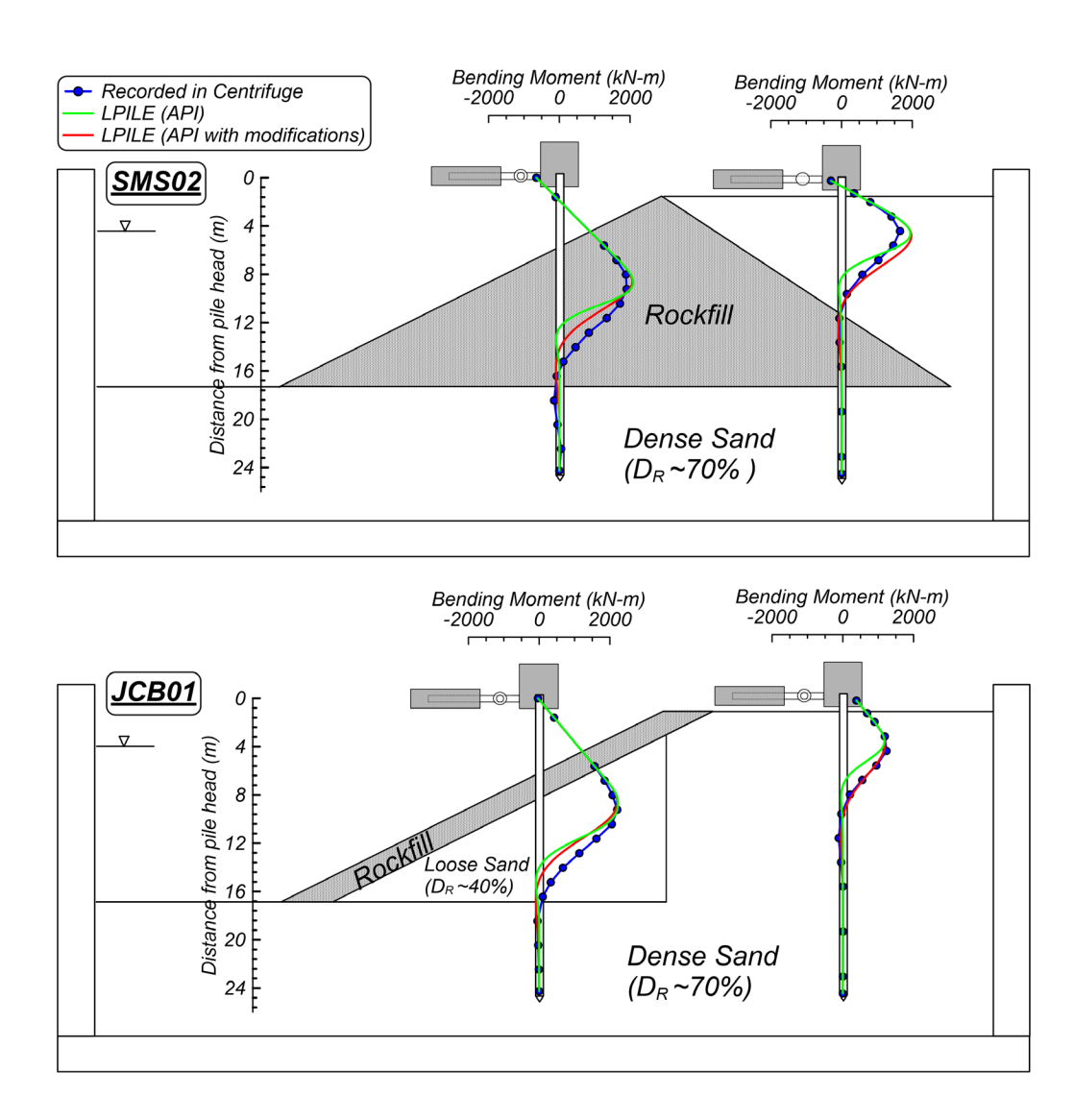


Figure 6. Comparison of recorded and predicted bending moments for static piles in SMS02 and JCB01

are shown for a case using the original API sand curves and a case with the modifications discussed earlier (i.e., reduced stiffness in all soil layers and a pseudo cohesion of 15 kPa in rockfill). While both models capture the maximum bending moment reasonably well, the model with reduced stiffness better captures the bending moment profile with depth as well as the maximum shear, soil reaction and pile displacement. Similar comparisons were made for the back pile in JCB01 and the back and front piles in SMS02. Figure 6 shows the bending moment comparisons between measured and estimated values using LPILE for all four static piles in both tests. The results shown in this figure confirm that the modifications made to API input parameters improve the predictions of the bending moment profiles, although it does not change the magnitude of the maximum moment along the pile.

Figure 7 shows the comparison of measured and predicted pile head load—displacement response in both the back and front piles in SMS02 and JCB01. As shown in this figure, the predicted pile head responses are in good agreement with the

responses back-calculated from the centrifuge tests (the secant stiffness in the models with *LPILE* with modification is up to 15% softer than the original *LPILE* results (e.g. JCB01, static back pile, bayward direction.) It is observed that the two *LPILE* models (with and without modifications) do not vary significantly in predicting the pile head response for the static piles. However, it will be shown later that using these modifications significantly improves the prediction of the bending moments for dynamic piles.

Experimental P-Y Curves from Dynamic Piles

Experimental p-y curves were also derived from centrifuge tests for piles supporting the wharf deck. These piles were subjected to wharf inertia during shaking, combined with varying magnitudes of ground deformation induced by partial/full liquefaction and slope instability. These dynamic p-y curves were then compared to the static p-y curves to investigate the effects of excess pore water pressure in liquefiable soils on the lateral response of piles and p-y curves.

8 | DFI JOURNAL | VOL. 14 | ISSUE 1

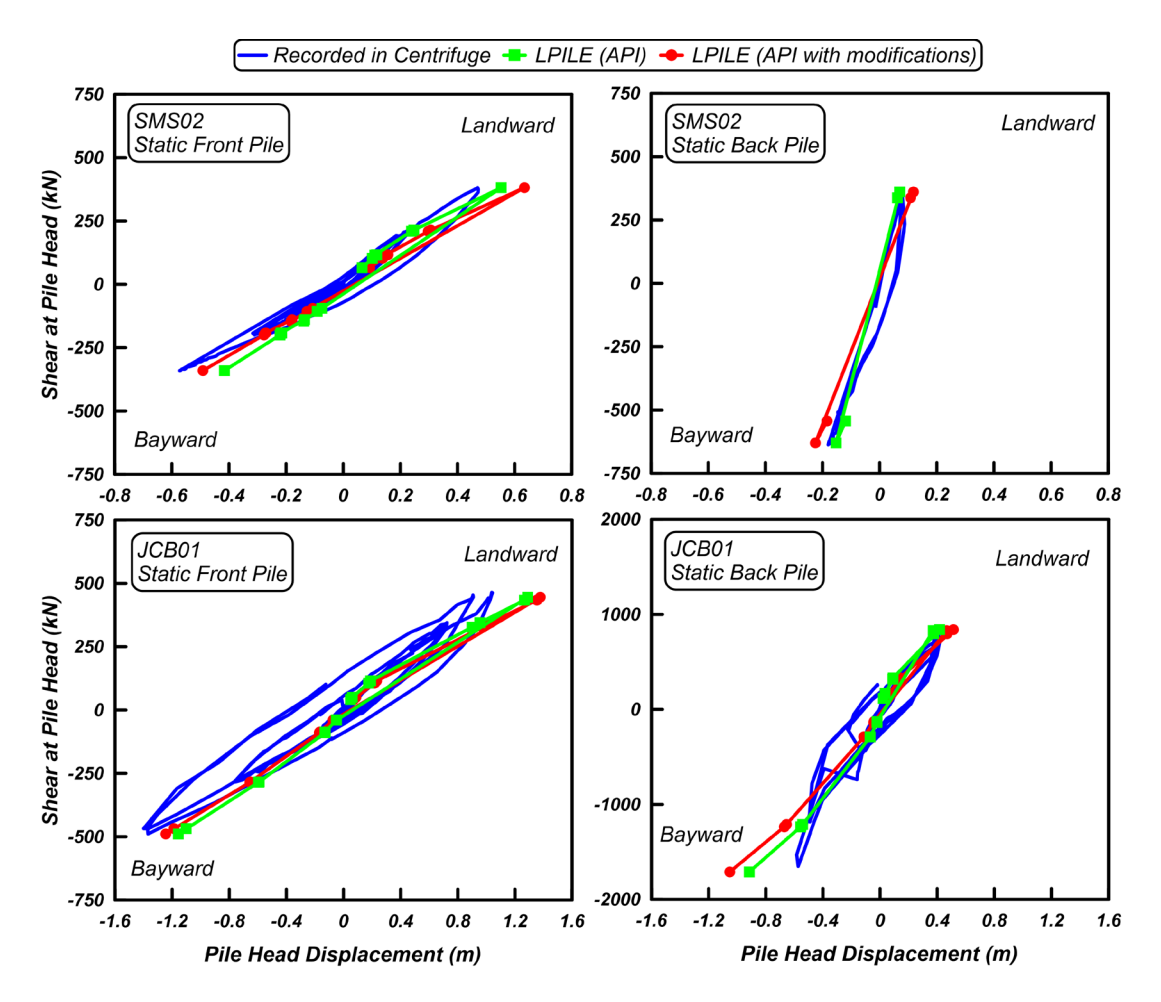


Figure 7. Comparison of recorded and predicted pile head load-displacement response for the static piles in JCB01 and SMS02

Figure 8 presents a comparison of static versus dynamic p-y curves for loose sand ($D_R = 40\%$). The static p-y curve shown in this figure was derived from the front static pile in JCB01 (the same curve shown in Figure 2). The dynamic p-y curve was derived from Pile #3 in JCB01 during the first earthquake motion. Both static and dynamic p-y curves are extracted at the same depth (3.05 m below the ground surface) and normalized by the same pile diameter (0.64 m). Overlapped on Figure 8 are two API sand curves that approximate the p-y responses under static and dynamic conditions. The API sand curve for the static condition is developed using the input parameters in Table 1. The API sand curve for the liquefied condition was developed by modifying the static API curve using a p-multiplier (P_m) to approximately envelop the dynamic experimental p-y curve. The p-multiplier was adjusted until it was visually a best fit to the measured response, and in this case was calculated as 0.21. The p-multiplier approach accounts for the first-order effects of liquefaction on p-y behavior.

The experimental dynamic p-y behavior is complex and is affected by contraction and dilation of loose sand, the inertial demand from the superstructure during earthquake loading, as well as factors such as strain rate, stress condition, and

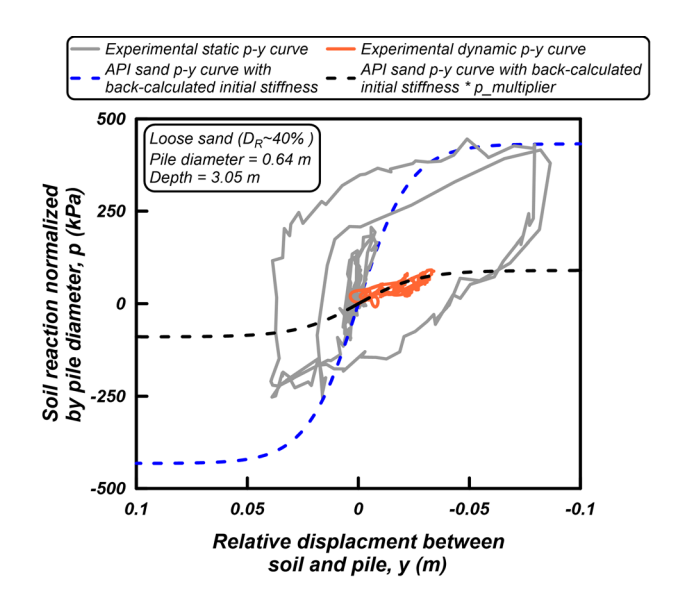


Figure 8. Comparison of static and dynamic p-y curves in loose sand in JCB01

ground slope. The last three cycles of loading for the experimental dynamic p-y curve presented in the previous figure are

plotted in Figure 9a using different colors to help understand the effect of the transient dilation of liquefied sand on the p-y response. The relative movement shown in Figure 9 is all in the bayward direction. The corresponding time windows for cycles A, B and C are shown with colored areas in the time histories in Figures 9b and 9c corresponding to the same colors shown earlier in Figure 9a for each cycle. These time histories illustrate the lateral soil resistance (p), relative lateral displacement between soil and pile (y), and excess pore water pressure ratio (R_{ij}) in the loose sand. It can be observed that as the excess pore water pressure ratio builds up in the loose sand in sloping ground, lateral spreading occurs that exerts lateral loads on the pile. It is also observed that the lateral soil reaction (p) in liquefied soil exhibits sudden spikes in the bayward direction as shown by the dashed lines. Careful examination of the spikes in p reveals that they follow transient drops in R_{μ} implying that they might be attributed to the dilative response of sand combined with an increase in the relative displacement between the soil and pile driven by the inertial demand from the wharf deck. However, the magnitude of the spikes in p are not very large (they are approximately 20% of P_{ult} of the static p-y curve), suggesting that a simple p-multiplier approach could be an effective choice for modifying the static p-y curve to represent the complex behavior of dynamic p-y curve in liquefied soil.

To further investigate the softening effect of liquefaction on the dynamic p-y curves, similar comparisons were made between the back-calculated static and dynamic p-y curves in loose sand as plotted in Figure 10. This figure includes static and dynamic p-y curves at depths of 5D and 7D below ground surface for Pile #3 and Pile #5 in JCB01 for two shaking events and at depth of 11D below ground surface for Pile #3 in NJM02 for one shaking event. These depths are selected because the loose sand layer was shallow enough that a direct comparison between static and dynamic p-y curves was possible. The p-multipliers were calculated as the ratio of the ultimate soil reaction in the dynamic curve to the ultimate soil reaction of the static p-y curve. For p-y curves at shallow depths (5D), p_{ult} is accurately captured by the API sand curve. However, for p-y curves at deeper locations (7D), the p_{ult} of the experimental stat-

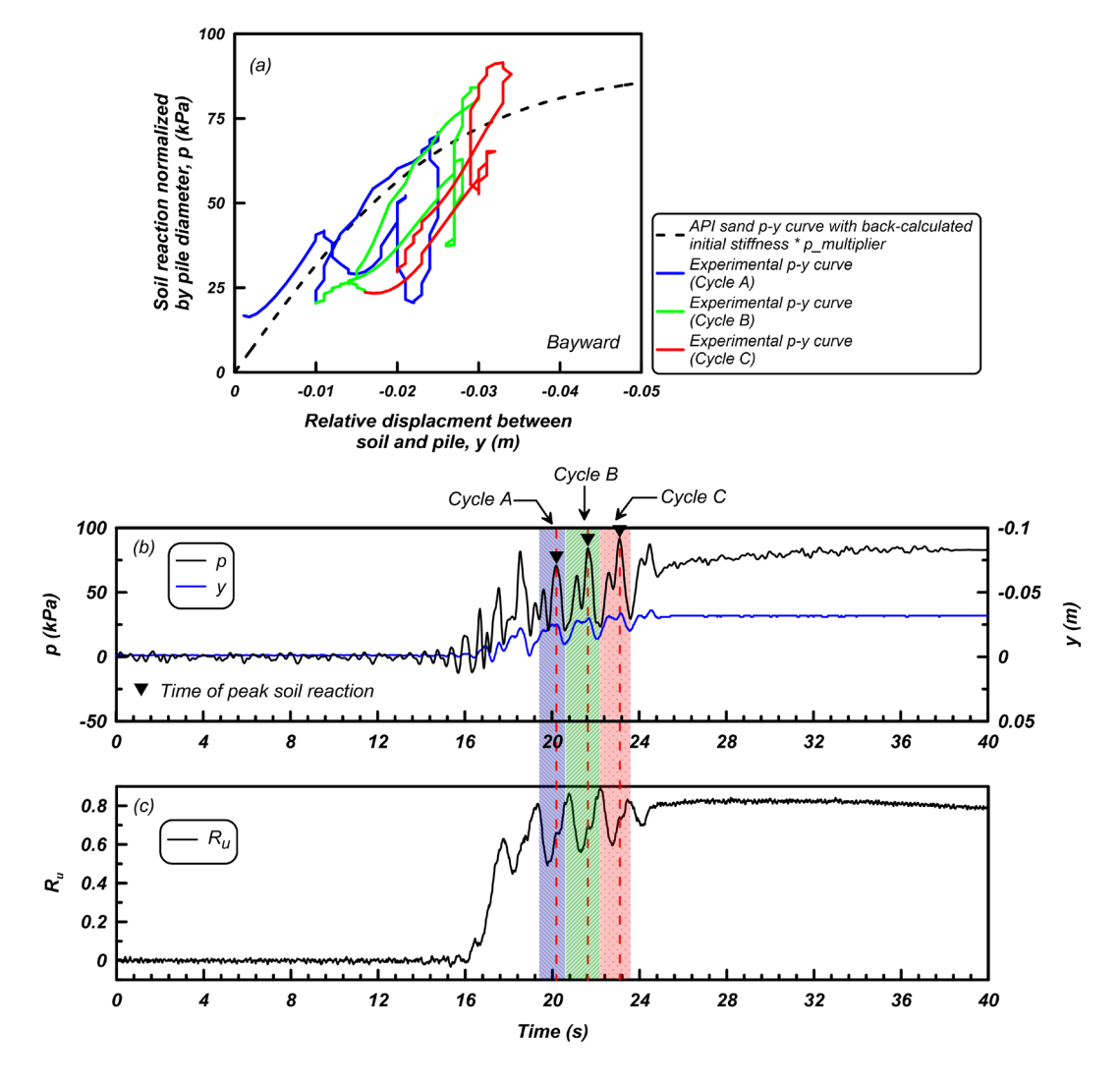


Figure 9. (a) Comparison of dynamic loading cycles in experimental p-y curve and modified API curve for liquefied sand; (b) Time histories of back-calculated soil reaction and relative soil-pile displacement; (c) Excess pore water pressure ratio measured in loose sand in JCB01

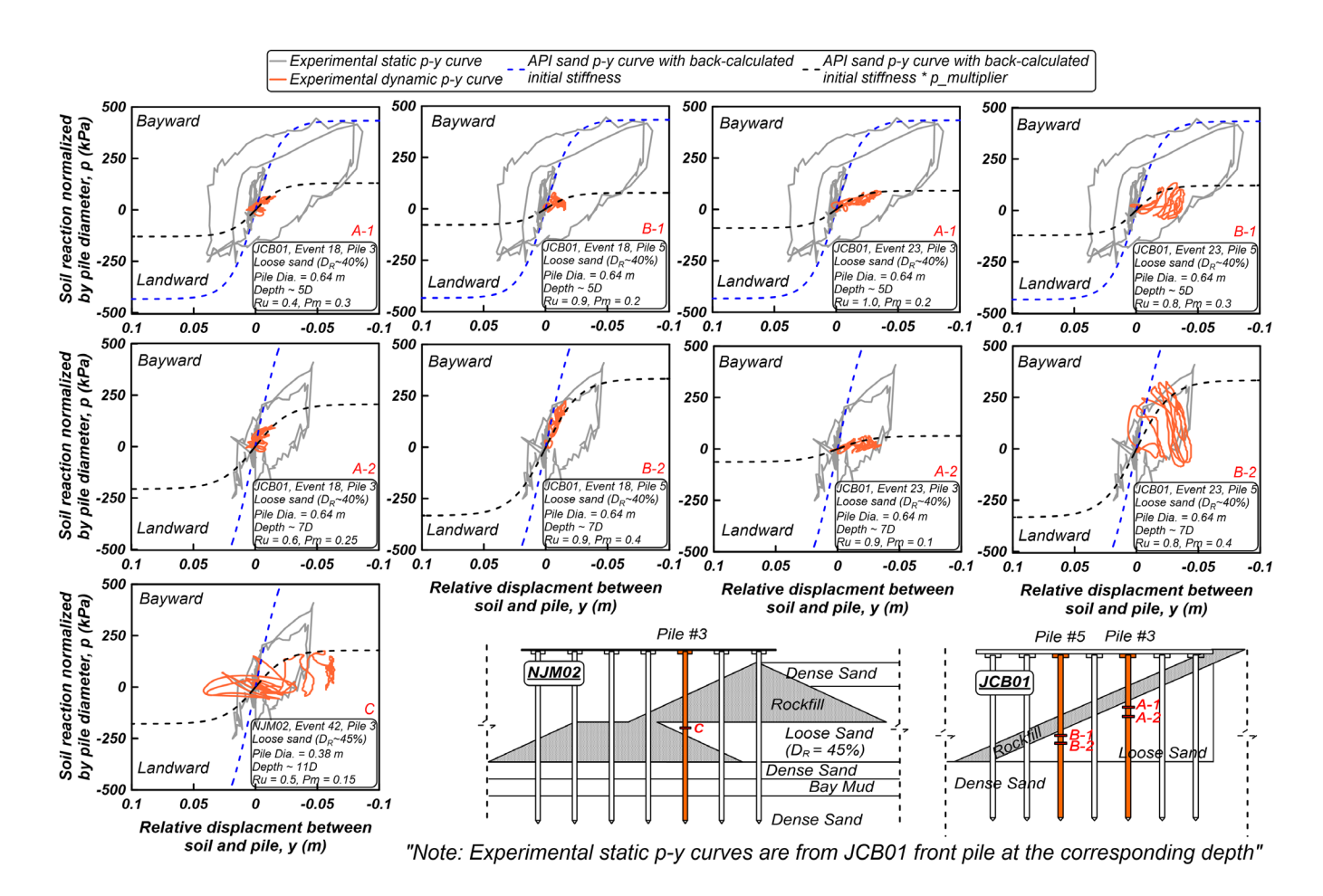


Figure 10. Comparison of static and dynamic p-y curves in loose sand at various depths

ic p-y curve is smaller than the p_{ult} of the API sand curve. This could be because the p_{ult} of the experimental static p-y curve is not yet mobilized at the displacements observed in the static tests at greater depths. Therefore, for these cases, the p-multipliers are divided by the p_{ult} from the API sand curve instead of the maximum soil reaction in the experimental static p-y curve.

Other researchers have shown that P_m values are correlated to the pore water pressure ratio (R_{y}) generated during shaking (e.g., Liu and Dobry 1995; Wilson et al. 2000; Brandenberg 2005; Chang and Hutchinson 2013). Figure 11 shows the back-calculated p-multipliers versus R_{μ} during dynamic shaking. The R_{μ} value was calculated using the pore pressure value from the transducer that was closest to the locations where the p-y curves were extracted. In practice, the pore water pressure can be estimated using advanced methods such as effective-stress dynamic analysis or simplified approaches where the excess pore water pressure ratio is correlated with the factor of safety against liquefaction (e.g. Marcuson at al. 1990). Also plotted in this figure are the data suggested by Liu and Dobry (1995) as presented in FHWA (2011). The data points for R₁ greater than 0.8 generally follow the data by Liu and Dobry. However, the three data points with R_{ij} between 0.4 to 0.6 exhibited p-multipliers that were approximately 0.15, which is much lower than those suggested by

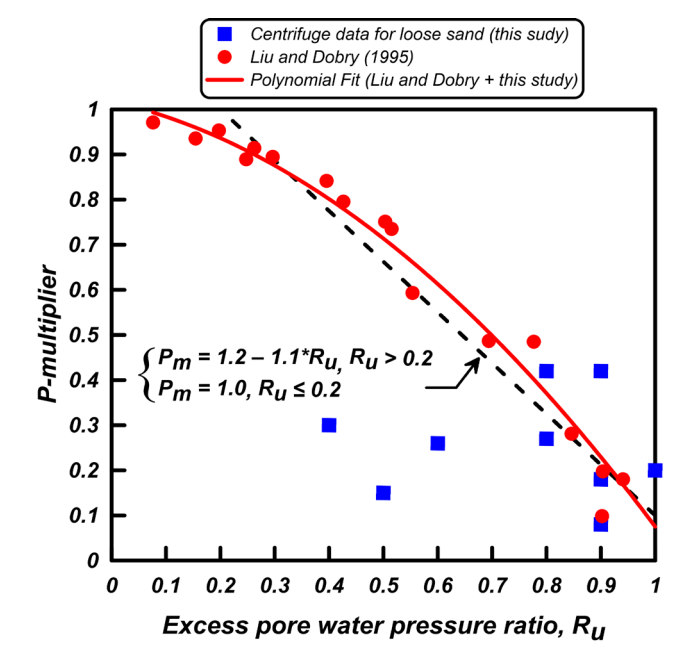


Figure 11. Comparison of back calculated p-multipliers from experimental p-y curves with excess pore water pressure ratio in loose sand and suggested data and relationship by Liu and Dobry (1995) as presented in FHWA (2011)

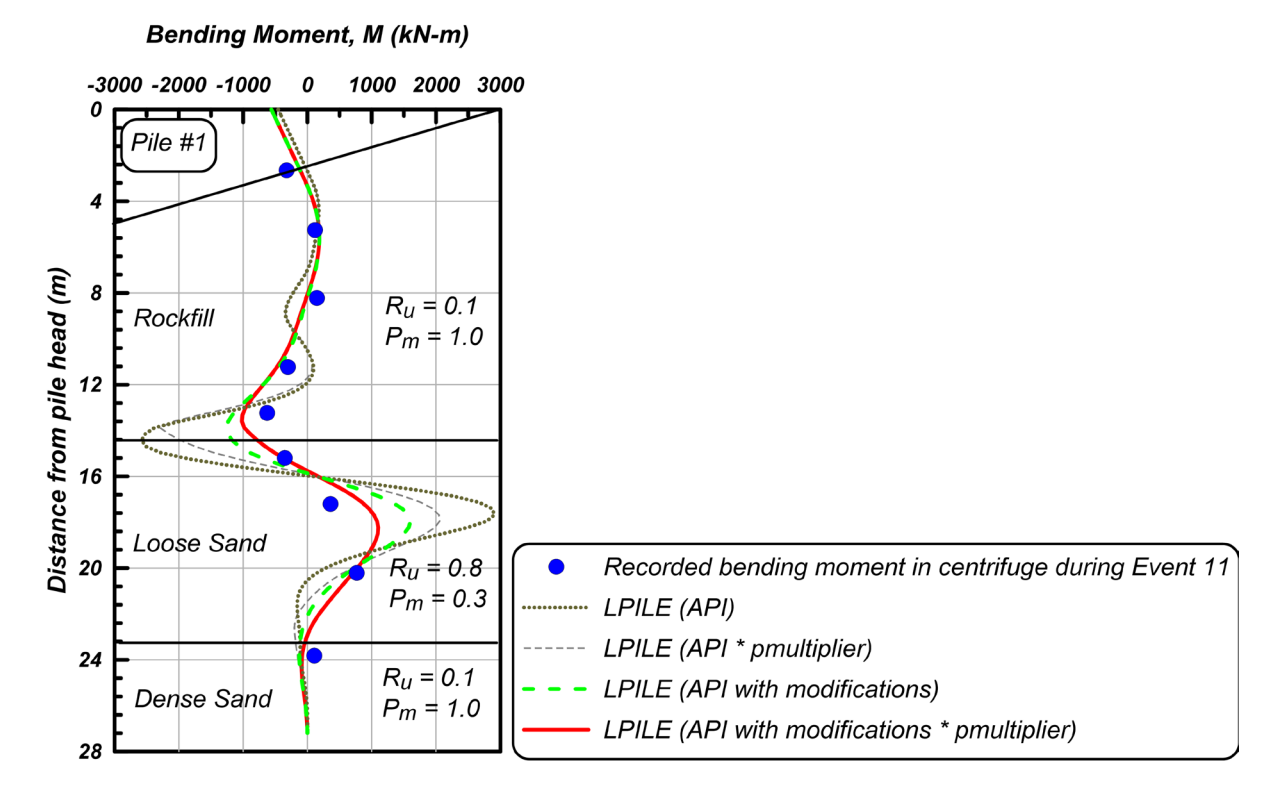
Liu and Dobry. These three cases correspond to the p-y curve shown for NJM02 and the two p-y curves from Event 18 for Pile 3 in JCB01. We hypothesize that close proximity to the highly permeable rockfill layers might have contributed in recording low R_{μ} in these three cases. Additionally, there is more uncertainty in the outlier data point for NJM02 because the p_{yh} of the experimental dynamic p-y curve may not have fully mobilized and there is significant amount of uncertainty in soil displacements as the shear failure plane passes through this location. More work is needed to explain the outlier cases observed in this study. The red line in this figure shows a polynomial fit to the data from Liu and Dobry (1995) combined with data from this study excluding the three outlier data points mentioned earlier. While the trend shows a nonlinear behavior, for simplicity, the p-multipliers in this study were calculated using $P_m = 1.2 - 1.1*R_u$ for $R_u > 0.2$ and P_m = 1.0 for $R_{y} \le 0.2$ as indicated by a dashed line in Figure 11. When R_{μ} is equal to 1.0, the p-multiplier is calculated as 0.1 and when R_{μ} is lower than 0.2 the effect of liquefaction is assumed to be negligible and the p-multiplier is calculated as 1.0. The R_u threshold of 0.2 corresponds approximately to a factor of safety against liquefaction (FS_{lid}) of 1.4 based on the laboratory test data on granular material by Marcuson at al. (1990). This linear fit was found to be a practice-oriented simplification and the effectiveness of this approach in estimating the pile demands is investigated next.

Validation Against Pile Demands

The effectiveness of the back-calculated input parameters for the API sand curves and the R_n -proportional p-multipli-

ers in liquefiable soils in predicting the lateral response of dynamic piles is investigated by comparing the pile bending moment profiles measured in the centrifuge tests to those estimated using p-y models in LPILE. The LPILE models consider combined kinematic and inertial effects, in which the soil displacements were imposed to the end nodes of the p-y springs and wharf inertia was imposed by a shear force at the pile head. The kinematic demands (i.e., soil displacements) and inertial demands (i.e., pile head shear) were directly calculated from the centrifuge tests at the exact time when the bending moments are at their peak values. The p-y curves were developed for each soil unit based on the API relationships with the input parameters listed in Table 1. The p-y curves were then softened using p-multipliers correlated to the R_u value using the linear equation described above $P_m = 1.2 - 1.1 * R_u$ for $R_u > 0.2$ and $P_m = 1.0$ for $R_u \le$ 0.2.

Figure 12 shows a comparison of the bending moments obtained from the first shaking event in Pile #1 in NJM01 (as a representative case) to those estimated from the LPILE analyses. The LPILE analyses were performed for four cases to evaluate the effectiveness of the modifications to the p-y curve and the application of a p-multiplier in predicting the pile bending moments in a liquefied layer. The best agreement between the measured and predicted pile bending moments was observed in the case where the initial stiffness of the API curve used the back-calculated stiffness values listed in Table 1 and the p-y curves were modified by p-multipliers that are a function of the R_u value in granular materials. As expected, the predicted bending moments



12 | DFI JOURNAL | VOL. 14 | ISSUE 1

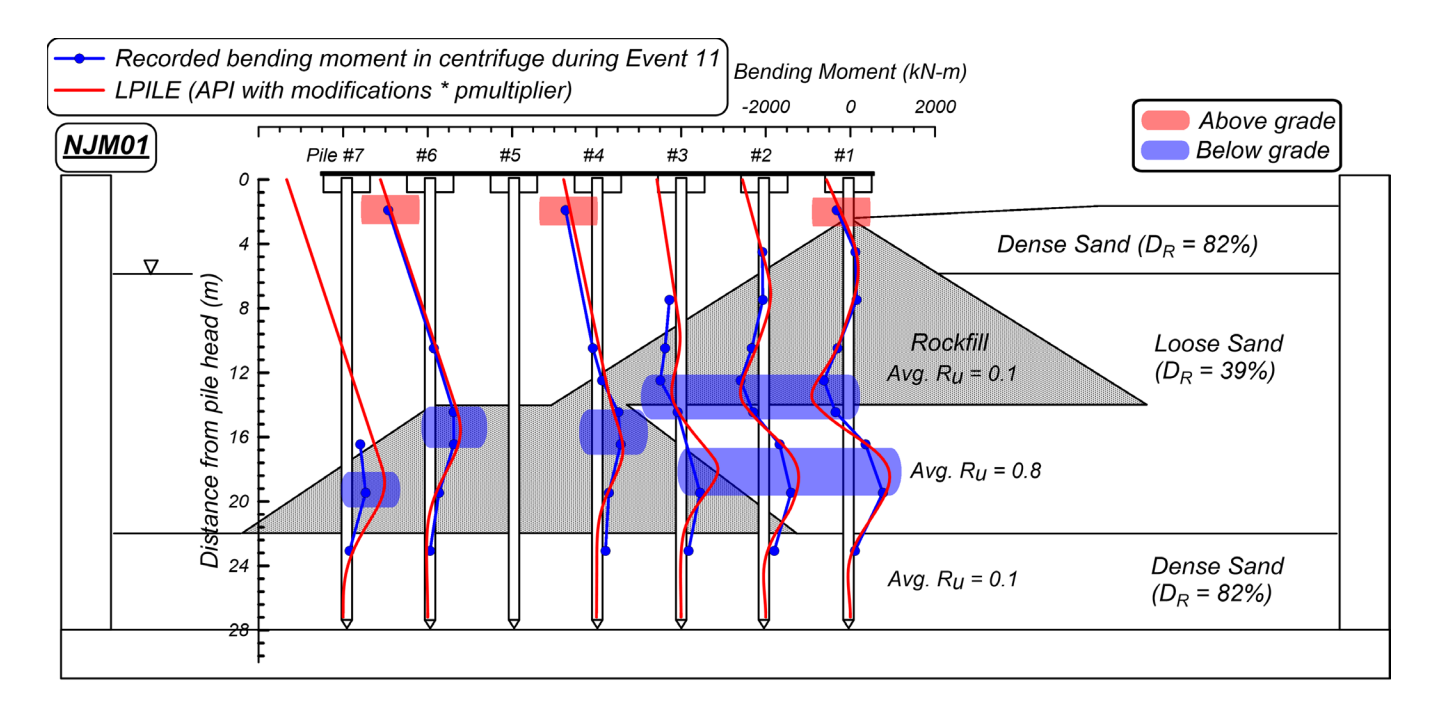


Figure 13. Comparison of recorded and estimated maximum bending moments for all instrumented dynamic piles in NJM01

without applying *p*-multipliers or without reducing the stiffness overestimated the demands. Similar observations can be made for other piles shown in the layout in Figure 13, in which the locations where large bending moments were observed are color-coded: bending moments above grade are shown in red, and those below grade are shown in blue. A comparison of the bending moments at these locations confirms that the simple *p*-multiplier approach is a reasonable approached to approximate the softer response of p-y curves in fully/partially liquefied zones.

In order to further investigate the applicability of the modified API curves, similar analyses were performed for the piles in all the five centrifuge tests. Figure 14 compares the peak bending moments in each instrumented pile from the centrifuge tests to the corresponding bending moments predicted using LPILE. It can be observed that bending moments can be reasonably predicted in piles subjected to liquefaction and lateral spreading loads using the modifications made to the API sand p-y curves. The majority of the peak bending moments from the centrifuge tests occurred when the wharf deck was moving in the bayward direction. In Figure 14, the bending moments below the mudline are plotted in blue and those above the mudline (at the pile head) are plotted in red. On average, the estimated bending moments using LPILE are 5% larger than the measured bending moments while the majority of the data points are bounded within the 1:2 and 2:1 lines (with the exception of two data points are very small bending moments). It can be seen that the p-y models were more accurate in estimating the bending moments at the pile head; however, the accuracy relies on the confidence in the estimation of the inertial demand (pile head shear) and kinematic demand (soil displacements).

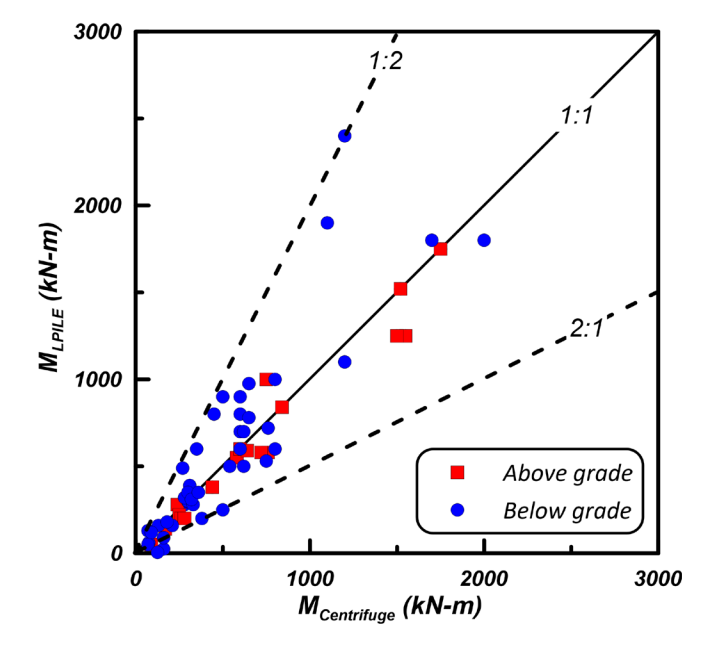


Figure 14. Comparison of maximum bending moments recorded from centrifuge and predicted from the *LPILE* analyses for all five centrifuge tests

Conclusions

The results of five centrifuge tests on pile-supported wharves in saturated sands were used to back-calculate representative static and dynamic p-y curves for laterally loaded piles. Two types of piles were used in this study: 1) single free-head piles with static cyclic lateral loads at the pile head prior to shaking, and 2) dynamic pile groups with fixed-head condition supporting the wharf deck and subjected to deck inertia loads and liquefaction-induced lateral spreading loads due to

earthquake ground shaking. The primary conclusions of the analyses are summarized as follows:

- Back-calculated p-y curves from static piles were approximated using API sand curves. The friction angles of 33°, 37° and 45° were used for loose sand ($D_p = 30\%$ to 40%), dense sand ($D_R = 70\%$ to 85%) and rockfill, respectively. These friction angles appeared to be adequate for estimating the ultimate lateral resistance (P_{ult}) of the experimental p-y curves, and the overall lateral response of the piles was adequately captured; therefore, no modifications were necessary. The initial stiffness values of the p-y curves that were back-calculated from the centrifuge tests. The back-calculated moduli of subgrade reaction were 3500 kN/m³, 3500 kN/m³, and 5200 kN/m³ for loose sand, dense sand and rockfill, respectively. These values are smaller than the values recommended by API (1993) which might be attributed to the aging effects between soils in the field and freshly deposited sands in the centrifuge tests and the effects of pile driving and installation in the field.
- When *p*-multipliers (P_m) in fully/partially liquefied zones were applied to the API sand curves, the softer response of the soils in liquefied zones was reasonably captured. The *p*-multipliers were calculated based on the excess pore water pressure ratio (R_u) generated during dynamic loading using a simple practice-oriented equation $(P_m = 1.2 1.1*R_u \text{ for } R_u > 0.2 \text{ and } P_m = 1.0 \text{ for } R_u \leq 0.2).$
- The comparison of the recorded pile bending moments and those estimated from LPILE demonstrates that the recommended modification of the API sand curves can reasonably predict the maximum pile bending moments in piles that are subjected to a complex combination of liquefaction-induced lateral spreading and superstructure inertial loading.
- The conclusions in this study were derived from the centrifuge tests performed on sands. The applicability of these conclusions to other types of soils that are prone to pore water pressure generation during cyclic loading (e.g. sandy silts and low-plasticity silts) need to be investigated in future studies

Acknowledgements

Support for conducting the centrifuge tests was provided by Grant No. CMS-9702744 from the National Science Foundation (NSF) and Grant No. SA2394JB from the Pacific Earthquake Engineering Research Center. Support for performing recent analyses on the centrifuge test results was provided by Grant No. CMMI-1761712 from NSF and Grant No. 171126 from the Deep Foundations Institute.

References

- Abdoun, T., Dobry, R., O'Rourke, T. D., and Goh, S. H. (2003). Pile response to lateral spreads: Centrifuge modeling. *Journal of Geotechnical and Geoenvironmental Engineering*, 129(10), 869–878.
- American Petroleum Institute, API (1993). Recommended practice for planning, design, and constructing fixed

- offshore platforms. API RP 2A-WSD, 20th Ed., API, Washington, D.C.
- Brandenberg, S. J., Boulanger, R. W., Kutter, B. L., and Chang, D. (2005). Behavior of pile foundations in laterally spreading ground during centrifuge tests. *Journal of Geotechnical and Geoenvironmental Engineering*, 131(11), 1378–1391.
- Brandenberg, S.J., Wilson, D.W., and Rashid, M.M., (2010). A Weighted Residual Numerical Differentiation Algorithm Applied to Experimental Bending Moment Data. *Journal of Geotechnical and Geoenvironmental Engineering*, 136(6), 854–863.
- Chang, B.J. and Hutchinson, T.C., (2013). Experimental evaluation of p-y curves considering development of liquefaction. *Journal of Geotechnical and Geoenvironmental Engineering*, 139(4), 577–586.
- LPILE. (2016). A program for the analysis of piles and drilled shafts under lateral loads. Version 2016.9.10 [computer program]. Austin, Texas: Ensoft Inc.
- Federal Highway Administration (FHWA) (2011). *LRFD* seismic analysis and design of transportation geotechnical features and structural foundations. Publication No. FHWA-NHI-11-032, GEC No. 3. Washington, D.C.: U.S. Department of Transportation.
- Franke, K.W. and Rollins, K.M. (2013). Simplified hybrid p-y spring model for liquefied soils. *Journal of Geotechnical and Geoenvironmental Engineering*, 139(4), 564–576.
- Haiderali, A. E., and Madabhushi, G. (2016). Evaluation of Curve Fitting Techniques in Deriving p--y Curves for Laterally Loaded Piles. *Geotechnical and Geological Engineering*, 34(5), 1453–1473.
- Liu, L., and Dobry, R. (1995). Effect of liquefaction on lateral response of piles by centrifuge model tests. NCEER Bulletin, 91, 7–11.
- Marcuson, W. F., Hynes, M. E., and Franklin, A. G. (1990). Evaluation and use of residual strength in seismic safety analysis of embankments, *Earthquake Spectra*, 6(3), 529–72.
- McCullough N. and Dickenson, S. (2004). The Behavior of Piles in Sloping Rock Fill at Marginal Wharves, *Proc. Ports* 2004, ASCE, May, Houston, TX.
- McCullough, N. J., Dickenson, S. E., & Schlechter, S. M. (2001). The seismic performance of piles in waterfront applications. In Ports' 01: America's Ports: Gateway to the Global Economy (pp. 1–10).
- McGann R, Arduino P, Mackenzie-Helnwein P. (2011). Applicability of conventional p—y relations to the analysis of piles in laterally spreading soil. *Journal of Geotechnical and Geoenvironmental Engineering*, 137(6):557–567.
- Rollins, K. M., Hales, L. J., Ashford, S. A., and Camp, W. M. (2005). P-Y curves for large diameter shafts in liq-

14 | DFI JOURNAL | VOL. 14 | ISSUE 1

- uefied sand from blast liquefaction tests. *ASCE Special Publication*: Seismic Performance and Simulation of Pile Foundations in Liquefied and Laterally Spreading Ground, 145, 11–23.
- Tokimatsu, K. (1999). Performance of pile foundations in laterally spreading soils. *Proc., 2nd Int. Conf. of Earth-quake Geotechnical Engineering*, P. S. Seco e Pinto, ed., Vol. 3, Balkema, Rotterdam, Netherlands, pp. 957–964.
- Wang, S-T., and Reese, L. C. (1998). Design of pile foundations in liquefied soils. *Geotechnical earthquake engineering and soil dynamics III, Geotechnical Special Publication No.* 75, Vol. 2, P. Dakoulas, M. Yegian, and R. Holtz, eds., Reston, Va. 1331–1343.
- Wilson, D. W. (1998). Soil-Pile-Superstructure Interaction in Liquefying Sand and Soft Clay. Report No. UCD/CGM-

- 98/04 Ph.D. Dissertation, University of California at Davis, Department of Civil & Environmental Engineering, Davis, California.
- Wilson, D. W., Boulanger, R. W., and Kutter, B. L. (2000). Observed seismic lateral resistance of liquefying sand. *Journal of Geotechnical and Geoenvironmental Engineering*, 126(10), 898–906.
- Yang, E. K., Choi, J. I., Kown, S. Y., and Kim, M. M. (2011). Development of dynamic p-y backbone curves for a single pile in dense sand by 1 g shaking table tests. *J. Civ. Eng.*, 15(5), 813–821.
- Yoo, M. T., Choi, J. I., Han, J. T., and Kim, M. M. (2013). Dynamic p-y curves for dry sand by dynamic centrifuge tests. *J. Earthq. Eng.*, 17(7), 1082–1102.

DFI Journal Underwriters









